

Charged particle elliptic flow in p+p collisions at LHC energies in a transport model PACIAE

Dai-Mei Zhou¹, Yu-Liang Yan², Bao-Guo Dong², Xiao-Mei Li², Du-Juan Wang¹, Xu Cai¹ and Ben-Hao Sa^{1,2,3}

¹ *Institute of Particle Physics and Key Laboratory of Quark & Lepton Physics,*

Huazhong Normal University, Wuhan 430079, China

² *China Institute of Atomic Energy, P.O. Box 275 (18), Beijing 102413, China*

³ *CCAST (World Laboratory), P. O. Box 8730 Beijing 100080, China*

The parton and hadron cascade model PACIAE based on PYTHIA was used to investigate the charged particle elliptic flow in minimum bias pp collisions at the LHC energies. The strings were distributed randomly in the transverse ellipsoid of the pp collision system with major axis of R (proton radius) and minor axis of $R(1 - \xi)$ before parton rescattering. The charged particle elliptic flow as a function of the random number ξ and transverse momentum p_T were investigated. The calculated v_2/ε as a function of reaction energy increases monotonously with increasing reaction energy up to $\sqrt{s} \sim 7$ TeV and then turns to saturation. With the parton-parton cross section enlarges three times in parton rescattering, the rapidity integrated charged particle elliptic flow may reach 0.025 at $p_T \sim 2$ GeV/c in the minimum bias pp collisions at $\sqrt{s}=7$ TeV.

PACS numbers: 25.75.Dw, 24.10.Lx

Elliptic flow is the 2nd harmonic in fourier expansion of the particle momentum azimuthal distribution [1]

$$\frac{1}{2\pi} \frac{dN}{dp_T dy d\phi} = \frac{1}{2\pi} \frac{dN}{p_T dp_T dy} [1 + 2 \sum_n v_n \cos n(\phi - \phi_R)]. \quad (1)$$

In theoretical studies the elliptic flow is calculated by

$$v_2 = \langle \overline{[\frac{p_x^2 - p_y^2}{p_T^2}]} \rangle, \quad (2)$$

where \overline{O} indicates an average of operator O over particles in an event and $\langle O \rangle$ an average over events [2].

The elliptic flow was suggested in hydrodynamic calculations [3] as a signature of collective expansion in the relativistic nuclear collisions. The consistency between experimental data of $v_1(y)$ as well as $v_2(p_T)$ at mid-rapidity and the corresponding hydrodynamic predictions was regarded as an evidence of the production of partonic matter in relativistic nucleus-nucleus collisions [4, 5]. The elliptic flow is now one of the most important observables in relativistic nucleus-nucleus collisions [6–9]. It has attracted high attention both experimentally and theoretically.

In non-central collision the reaction zone (overlap region) between two colliding nuclei is spatially asymmetric. The rescattering process among the produced particles transfers this spatial asymmetry into the momentum space, and the momentum distribution of the produced particles becomes azimuthally anisotropic. This picture is generally valid for a large system. In the pp collision at RHIC energy, the average multiplicity $\langle n_{ch} \rangle$ is not big enough for collective effects to be detected. However, in the pp collisions at $\sqrt{s}=7$ TeV, it has already been observed that the multiplicity can reach $\frac{dN_{ch}}{d\eta} > 30$ [10, 11]. Therefore the elliptic flow may be measurable in the pp collision at LHC energies and the further theoretical studies are also required.

The fluctuations in pp interaction region can result in a sizable spatial eccentricity was assumed in [12]. With further assumptions on the nature of this fluctuations and on the eccentricity scaling of elliptic flow, they reported that the elliptic flow becomes measurable in high-multiplicity pp collisions at LHC energies. The initial interactions produce a number of hot spots was assumed in [13]. Their hydrodynamical evolution of two or more hot spots generated a sufficiently large elliptic flow. In [14] a Monte Carlo implementation of the dipole (gluon) cascade model was introduced to study the elliptic flow in pp collision at LHC energies. They predicted that v_2 in $\sqrt{s}=7$ TeV pp collision is around 6-7%. The ideal 3+1D hydrodynamic simulation was used to study the v_2 in [15], and they concluded that the elliptic flow can occur at least for top multiplicities pp collision at $\sqrt{s}=14$ TeV. In [16] the hydrodynamic model calculations showed that if high multiplicity events in the pp collisions at LHC energies contain two flux tubes, the elliptic flow may be observable. Many other models also gave their predictions [17].

We studied the charged particle elliptic flow in minimum bias pp collisions at the LHC energies by a parton and hadron cascade model PACIAE [18] based on PYTHIA [19] in this letter. It is well known that PYTHIA is a model for high energy hadron-hadron (hh) collisions. In the PYTHIA model a hh collision is decomposed into the parton-parton collisions. A hard parton-parton collision is described by the lowest leading order perturbative QCD (LO-pQCD). The soft parton-parton collision is considered empirically. Because the initial- and final-state QCD radiations and multiparton interactions are considered in the parton-parton scattering, the consequence of a hh collision is a parton multijet configuration composed of di-quarks (anti-diquarks), quarks (anti-quarks), and gluons, besides a few hadronic remnants. This parton multijet configuration is followed by the string construction and fragmentation (hadronization). Therefore one obtains a hadronic final state for a hh (pp) collision.

For pp collisions the PACIAE model is different from PYTHIA in the addition of the parton rescattering before hadronization and the hadron rescattering after hadronization. The PACIAE model consists of the parton initialization, parton evolution (rescattering), hadronization, and hadron evolution (rescattering) four stages.

1. The parton initialization:

The parton initialization is performed by the PYTHIA model with string fragmentation (hadronization) switched-off. One obtains a parton configuration composed of quarks, anti-quarks, and gluons, besides a few hadronic remnants for a pp (hh) collision after diquarks (anti-diquarks) being split randomly into quarks (anti-quarks). This parton configuration is regarded as quark-gluon matter (QGM) formed in the initial state (fireball) of pp collision.

2. The parton evolution (rescattering):

The rescattering among partons in QGM is then considered by the $2 \rightarrow 2$ LO-pQCD parton-parton cross sections [20]. The differential cross section of a subprocess $ij \rightarrow kl$ is

$$\frac{d\sigma_{ij \rightarrow kl}}{d\hat{t}} = K \frac{\pi\alpha_s^2}{\hat{s}} \sum_{ij \rightarrow kl}, \quad (3)$$

where the factor K (assumed to be 3 in this letter) is introduced considering the higher order and the nonperturbative corrections, $\alpha_s=0.47$ stands for the effective strong coupling constant, and \hat{s} , \hat{t} , as well as \hat{u} refer to the Mandelstam variables. The specific subprocess $q_1\bar{q}_2 \rightarrow q_1\bar{q}_2$, for instance, has

$$\sum_{q_1\bar{q}_2 \rightarrow q_1\bar{q}_2} = \frac{4}{9} \frac{\hat{s}^2 + \hat{u}^2}{\hat{t}^2}. \quad (4)$$

It is regularized by introducing the parton color screen mass μ ($=0.63$ GeV) as

$$\sum_{q_1 \bar{q}_2 \rightarrow q_1 \bar{q}_2} = \frac{4}{9} \frac{\hat{s}^2 + \hat{u}^2}{(\hat{t} - \mu^2)^2}. \quad (5)$$

The total cross section of $i + j$ parton collision is then

$$\sigma_{ij}(\hat{s}) = \sum_{k,l} \int_{-\hat{s}}^0 d\hat{t} \frac{d\sigma_{ij \rightarrow kl}}{d\hat{t}}. \quad (6)$$

With the total and differential cross sections above the parton evolution (rescattering) can be simulated by the Monte Carlo method until all parton-parton collisions are exhausted (partonic freeze-out). The results introduced later were calculated using this pQCD cross sections except special mention.

3. The hadronization:

In the hadronization stage, the partonic matter (QGM) formed after parton rescattering is hadronized by the Lund string fragmentation regime [19] after string reconstruction or by the Monte Carlo coalescence model. The former model has been described in detail in [19]. We proposed a phenomenological coalescence model for the later one [18]. In this model, two partons coalesce a meson and three partons a baryon (antibaryon) according to the valence quark structure of hadron and the flavors, positions as well as the momenta of coalescing partons. The positions and momenta of coalescing partons are constrained to the phase space requirement

$$\frac{16\pi^2}{9} \Delta r^3 \Delta p^3 = \frac{h^3}{d} \quad (7)$$

where h^3/d is the volume occupied by a single hadron in the phase space, $d=4$ refers to the spin and parity degeneracies of the hadron, Δr and Δp stand for the position and momentum distances between coalescing partons, respectively. In addition, the momenta of coalescing partons have to satisfy the momentum conservation.

4. The hadron evolution (rescattering):

In this stage the hadronic matter after hadronization proceeds rescattering. It is dealt with by the usual two-body elastic and inelastic collisions [21], until the hh collision pairs are exhausted (hadronic freeze-out). The rescatterings among $\pi, K, p, n, \rho(\omega), \Delta, \Lambda, \Sigma, \Xi, \Omega, J/\Psi$ and their antiparticles are considered for the moment. The isospin averaged parametrization formula [22, 23] is assumed for cross section of hh collisions. In addition, an assumed constant total cross sections ($\sigma_{\text{tot}}^{NN} = 40$ mb, $\sigma_{\text{tot}}^{\pi N} = 25$ mb, $\sigma_{\text{tot}}^{KN} = 20$ mb, and $\sigma_{\text{tot}}^{\pi\pi} = 10$ mb) and ratio of inelastic to total cross section (0.85) are provided as another option.

The PYTHIA and PACIAE models with default parameters (except the factor K was assumed to be 3) were used to generate pp minimum bias events at $\sqrt{s}=14$ TeV. We found that the charged particle $v_2(p_T)$ from the PYTHIA calculations was almost zero and the one from PACIAE was just around 0.0012. Following the idea of hot spots [12, 13, 16] we assumed that the strings before parton rescattering were distributed randomly in the transverse elliptic zone of the pp collision system. The major and minor axes of this ellipsoid were

$$a = R, \quad (8)$$

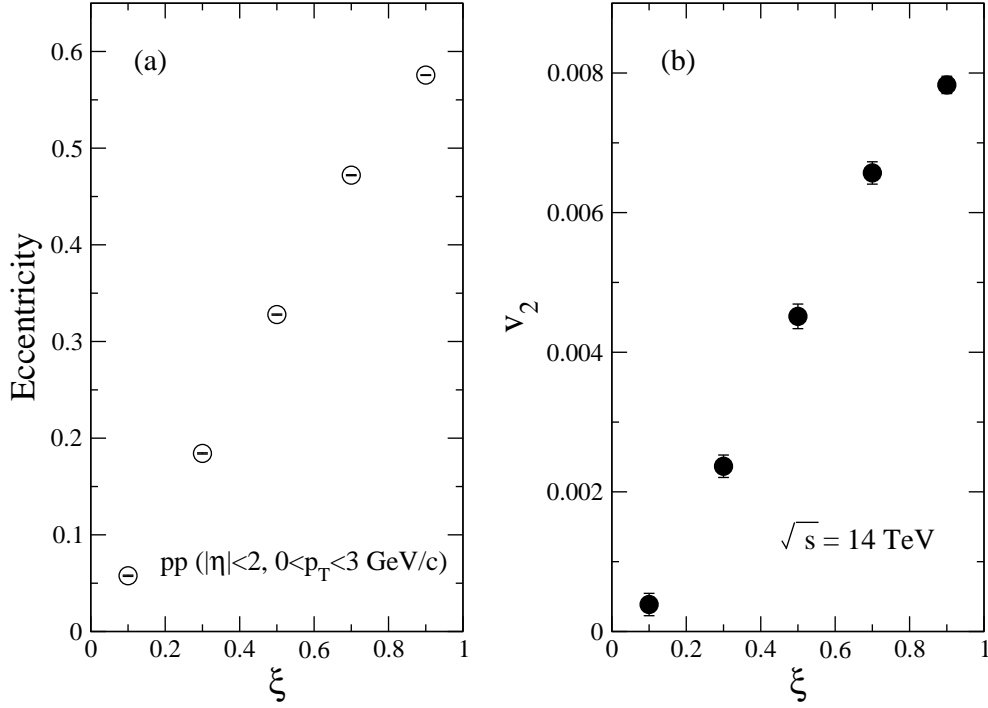


FIG. 1: Charged particle eccentricity and elliptic flow as a function of ξ in minimum bias pp collision at $\sqrt{s}=14 \text{ TeV}$.

and

$$b = R(1 - \xi), \quad (9)$$

respectively. In above equations R was the radius of proton and the parameter ξ (random number) reflects the fluctuation in the initial position distribution in pp collision. The constituent partons in a string were sampled randomly in a circle centered at the string and with radius of 1 fm.

We calculated the charged particle eccentricity [24]

$$\langle \varepsilon \rangle = \left\langle \frac{\sigma_y^2 - \sigma_x^2}{\sigma_y^2 + \sigma_x^2} \right\rangle \quad (10)$$

according to parton initial state in position space (later it was simply indicated as ε). In this equation $\sigma_x^2 = \overline{x^2} - \overline{x}^2$ and $\sigma_y^2 = \overline{y^2} - \overline{y}^2$ were the variance of the initial parton distribution in the x and y directions in a given event.

Figure 1 (a) and (b) give the charged particle eccentricity and the integrated elliptic flow v_2 ($|\eta| < 2$ and $0 < p_T < 3 \text{ GeV}/c$) as a function of ξ in the minimum bias pp collisions at $\sqrt{s}=14 \text{ TeV}$ in the PACIAE calculations, respectively. Both the eccentricity and elliptic flow increase with increasing ξ that may mean the integrated v_2 is proportional to the initial eccentricity as expected in [25].

The charged particle integrated elliptic flow v_2 as a function of the transverse momentum p_T in minimum bias pp collisions at $\sqrt{s}=14 \text{ TeV}$ is given in Fig.2. In this figure the full circles, squares, and triangles are the results calculated with $\xi=0.1, 0.5$, and 0.9 , respectively. The v_2 value increases with increasing ξ that may represent the final momentum asymmetry is originated from initial position anisotropy.

Figure 3 shows the reaction energy dependence of scaled elliptic flow v_2/ε in the minimum bias pp collisions calculated with $\xi = 0.9$. In this figure v_2 is integrated over η and p_T . One sees here that v_2/ε increases with

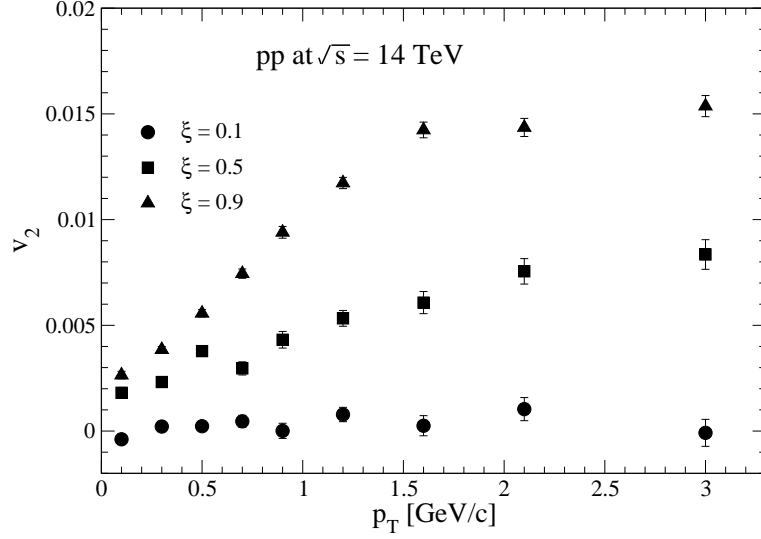


FIG. 2: Charged particle v_2 as a function of p_T in minimum bias pp collisions at $\sqrt{s}=14$ TeV.

increasing reaction energy monotonously up to 7 TeV and then turns to saturation. This behavior is similar to v_2/ϵ varies with centrality observed in relativistic heavy ion collisions reported in [26].

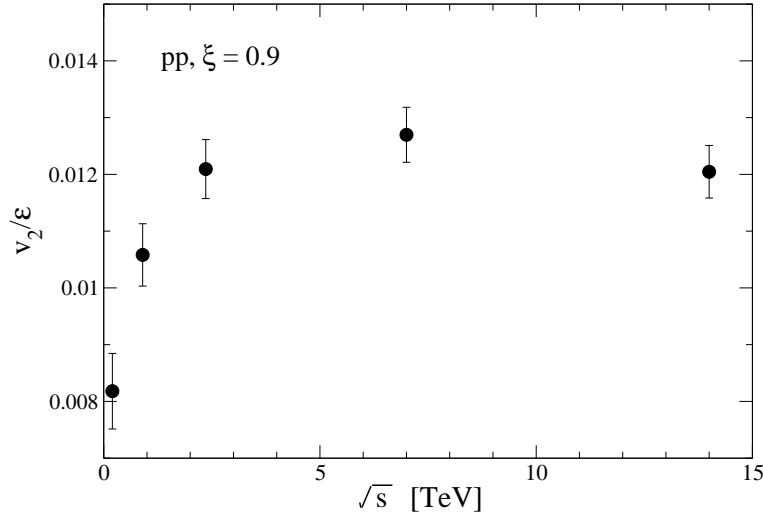


FIG. 3: The scaled charged particle elliptic flow, v_2/ϵ , as a function of collision energy in minimum bias pp collisions .

The function of charged particle integrated elliptic flow v_2 versus transverse momentum p_T varying with parton-parton interaction cross section in the minimum bias pp collision at $\sqrt{s}=14$ TeV calculated with $\xi=0.9$ is shown in Fig. 4. The full circles are the results calculated by the pQCD parton-parton cross sections in the parton rescattering while the full squares are calculated by three times enlarged parton-parton cross sections. We see in this figure that the charged particle integrated elliptic flow increases nearly 60% at $p_T \sim 2$ GeV/c if the parton-parton cross section

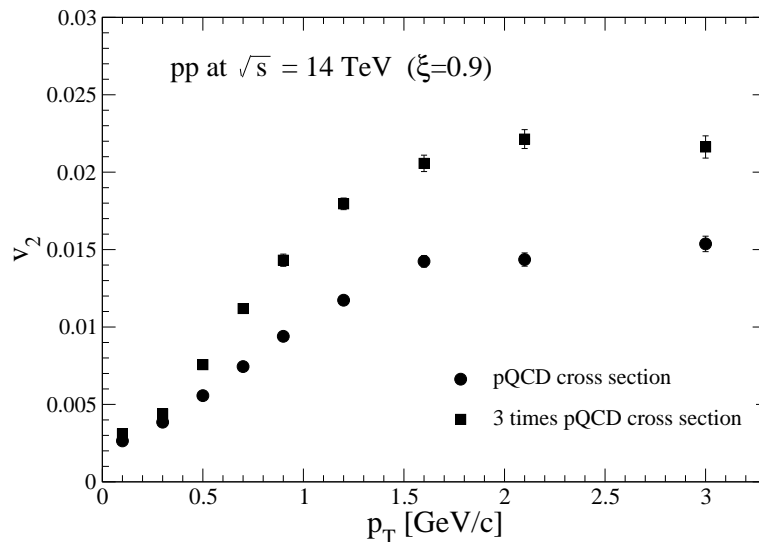


FIG. 4: Charged particle elliptic flow v_2 as a function of the transverse momentum p_T in minimum bias pp collision at $\sqrt{s}=14$ TeV with two different parton-parton cross sections.

is increased by three times. That indicates the importance of the parton rescattering.

In summary, the parton and hadron cascade model PACIAE was used to study the charged particle elliptic flow in the minimum bias pp collisions at LHC energies. The strings were distributed randomly in the transverse ellipsoid of the pp collision system with major axis of R (proton radius) and minor axis of $R(1 - \xi)$ before parton rescattering. We investigated the charged particle elliptic flow as a function of the random number ξ and transverse momentum p_T , respectively. The calculated v_2/ε as a function of reaction energy first increases monotonously with increasing reaction energy up to $\sqrt{s} \sim 7$ TeV and then turns to saturation. We find that the parton rescattering is also very important. If the parton-parton cross section enlarges three times, the rapidity integrated charged particle elliptic flow v_2 increases nearly 60% and reach to 0.025 at $p_T \sim 2$ GeV/c in the minimum bias pp collisions at $\sqrt{s}=7$ TeV.

Acknowledgments

The financial supports from NSFC (10975062, 11075217, 11047142, 10705012) and from the Commission on Higher Education in China are acknowledged.

-
- [1] A. M. Poskanzer and S. A. Voloshin, Phys. Rev. C **58**, 1671 (1998).
 - [2] Xiao-Mei Li, Bao-Guo Dong, Yu-Liang Yan, Hai-Liang Ma, Dai-Mei Zhou, and Ben-Hao Sa, Modern Phys. lett. **A25**, 1211 (2010).
 - [3] J. Y. Ollitrault, Phys. Rev. D **46**, 229 (1992).
 - [4] M. Gyulassy, arXiv:nucl-th/0403032, and in “Structure and dynamics of elementary matter”: Proceedings of the NATO Advanced Study Institute on Structure and Dynamics of Elementary Matter, Camyuva-Kemer (Antalya), Turkey, 22 September-2 October 2003, ed. by W. Greiner .

- [5] L.P. Csernai and D. Röhrich, Phys. Lett. **B 458** (1999) 454.
- [6] K. H. Ackerman et al., STAR Collaboration, Phys. Rev. Lett. **86**, 402 (2001).
- [7] S. S. Adler et al., PHENIX Collaboration, Phys. Rev. Lett. **91**, 182301 (2003).
- [8] B. Alver et al., PHOBOS Collaboration, Phys. Rev. Lett. **98**, 242302 (2007).
- [9] ALICE Collaboration, arXiv:1011.3914.
- [10] K. Aamodt et al., ALICE Collaboration, Eur. Phys. J. C **68**, 345 (2010).
- [11] CMS Collaboration, JHEP09 091 (2010).
- [12] Jorge Casalderrey-Solana and Urs Achim Wiedemann, Phys. Rev. Lett. **104**, 102301 (2010).
- [13] A. K. Chaudhuri, Phys. Lett. B **692**, 15 (2010).
- [14] Emil Avsar et al., arXiv:1009.5643v2.
- [15] G. Ortona et al., arXiv:0911.5158v1.
- [16] P. Bozek, Acta Phys. Polon. B **41**, 837 (2010).
- [17] L. Cunqueiro, J. Dias de Deus, and C. Pajares, Eur. Phys. J. C **65**, 423 (2010); M. Luzum and P. Romatschke, Phys. Rev. Lett. **103**, 262302 (2009) ; D. d'Enterria et al., Eur. Phys. J. C **66**, 173 (2010).
- [18] Most recent references: Ben-Hao Sa, Dai-Mei Zhou, Bao-Guo Dong, Yu-Liang Yan, Hai-Liang Ma, and Xiao-Mei Li, J. Phys. G: Nucl. Part. Phys. **36**, 025007 (2009); Yu-Liang Yan, Dai-Mei Zhou, Bao-Guo Dong, Xiao-Mei Li, Hai-Liang Ma, and Ben-Hao Sa, Phys. Rev. C **79**, 054902 (2009).
- [19] T. Sjöstrand, S. Mrenna, and P. Skands, J. High Energy Phys. **JHEP05**, 026 (2006).
- [20] B. L. Combridge, J. Kripfgang, and J. Ranft, Phys. Lett. B **70**, 234 (1977).
- [21] Ben-Hao Sa and Tai An, Comput. Phys. Commun. **90**, 121 (1995); Tai An and Ben-Hao Sa, Comput. Phys. Commun. **116**, 353 (1999).
- [22] P. Koch, B. Müller, and J. Rafelski Phys. Rep. **142**, 167 (1986).
- [23] A. Baldini, et al., "Total cross sections for reactions of high energy particles", Springer-Verlag, Berlin, 1988.
- [24] B. Alver, et al., Phys. Rev. C **77**, 014906 (2008).
- [25] J. Y. Ollitrault, Eur. J. Phys. **29**, 275 (2008).
- [26] H-J. Drescher, A. Dumitru, C.Gombeaud, and J-Y. Ollitrault, Phys. Rev. C **76**, 024905 (2007).